Available online at www.sciencedirect.com
SCIENCE DIRECT
Journal of Asian Earth Sciences 28 (2006) 469–479
Journal of Asian Earth Sciences
www.elsevier.com/locate/jaes

Palaeomagnetically defined rotations of fault-bounded continental blocks in the North Anatolian Shear Zone, North Central Anatolia

Turgay İşseven [a,*], Okan Tüysüz [b]

[a] Department of Geophysical Engineering, Faculty of Mines, Istanbul Technical University, 34469 Maslak, Turkey
[b] Eurasia Institute of Earth Sciences, Istanbul Technical University, 34469 Maslak, Turkey

Received 13 September 2004; received in revised form 31 October 2005; accepted 28 November 2005

Abstract

The 1200 km-long North Anatolian Transform Fault connects the East Anatolian post-collisional compressional regime in the east with the Aegean back-arc extensional regime to the west. This active dextral fault system lies within a shear zone reaching up to 100 km in width, and consists of southward splining branches. These branches, which have less frequent and smaller magnitude earthquake activity compare to the major transform, cut and divide the shear zone into fault delimited blocks. Comparison of palaeomagnetic data from 46 sites in the Eocene volcanics from different blocks indicate that each fault-bounded block has been affected by vertical block rotations. Although clockwise rotations are dominant as expected from dextral fault-bounded blocks, anticlockwise rotations have also been documented. These anticlockwise rotations are interpreted as due to anticlockwise rotation of the Anatolian Block, as indicated by GPS measurements, and the effects of unmapped faults or pre-North Anatolian Fault tectonic events.

Keywords: Palaeomagnetism; Eocene volcanics; Block rotations; Central Anatolia

1. Introduction

Turkey is represented by a tectonic collage of small continental fragments separated by suture zones (Fig. 1a). This orogenic collage developed from the closure of different branches of the Tethyan Ocean, formerly situated between Laurasia and Gondwana (Şengör and Yılmaz, 1981; Okay and Tüysüz, 1999). Final amalgamation of these fragments into a single continental mass occurred at ~11 Ma when the Arabian plate collided with the Anatolian plate (Şengör and Yılmaz, 1981). This collision also represents the end of the palaeotectonic period and the beginning of the neotectonic period of deformation of the Anatolian plate (Şengör, 1979, 1980). Following collision, a compressional tectonic regime has prevailed as the Arabian plate continued to move northward and cause thickening and uplift of Eastern Anatolia. The continuation of this compressional regime has also forced westward escape along two strike-slip faults, the Northern and the Eastern Anatolian Transform Faults, toward the Aegean back-arc extensional regime driven by trench rollback on the Hellenic Arc (Le Pichon and Angelier, 1979). Recent GPS measurements indicate that the Arabian plate still moves northward at a rate of 18 mm/y and Anatolia moves westwards at a rate of 24 mm/y (McClusky et al., 2000) along the North Anatolian Fault (NAF) and 9 mm/y along the Eastern Anatolian Fault. GPS measurements also indicate that the Anatolian Plate delimited by these two transform faults is rotating anticlockwise about an Eulerian pole in the Sinai Peninsula (McClusky et al., 2000).

The NAF, starting from Karlıova in the east and extending to the Gulf of Saros in the west, is a 1200 km-long dextral fault connecting the East Anatolian compressional regime to the Aegean extensional regime (Fig. 1b). Şengör et al. (2005) conclude that this fault is part of a dextral shear zone reaching up to 100 km in width, the North Anatolian Shear Zone (NASZ), where it is confined to the weak zone of the crust represented by the North Anatolian Tethyside accretionary complexes of latest Palaeozoic to early Tertiary age. The northern part of the North Anatolian Fault is located within the Pontides (Ketin, 1966). The shear zone itself consists of a

* Corresponding author. Fax: +90 212 285 6201.
E-mail addresses: isseven@itu.edu.tr (T. İşseven), tuysuz@itu.edu.tr (O. Tüysüz).

1367-9120/$ - see front matter © 2006 Elsevier Ltd. All rights reserved.
doi:10.1016/j.jseaes.2005.11.012

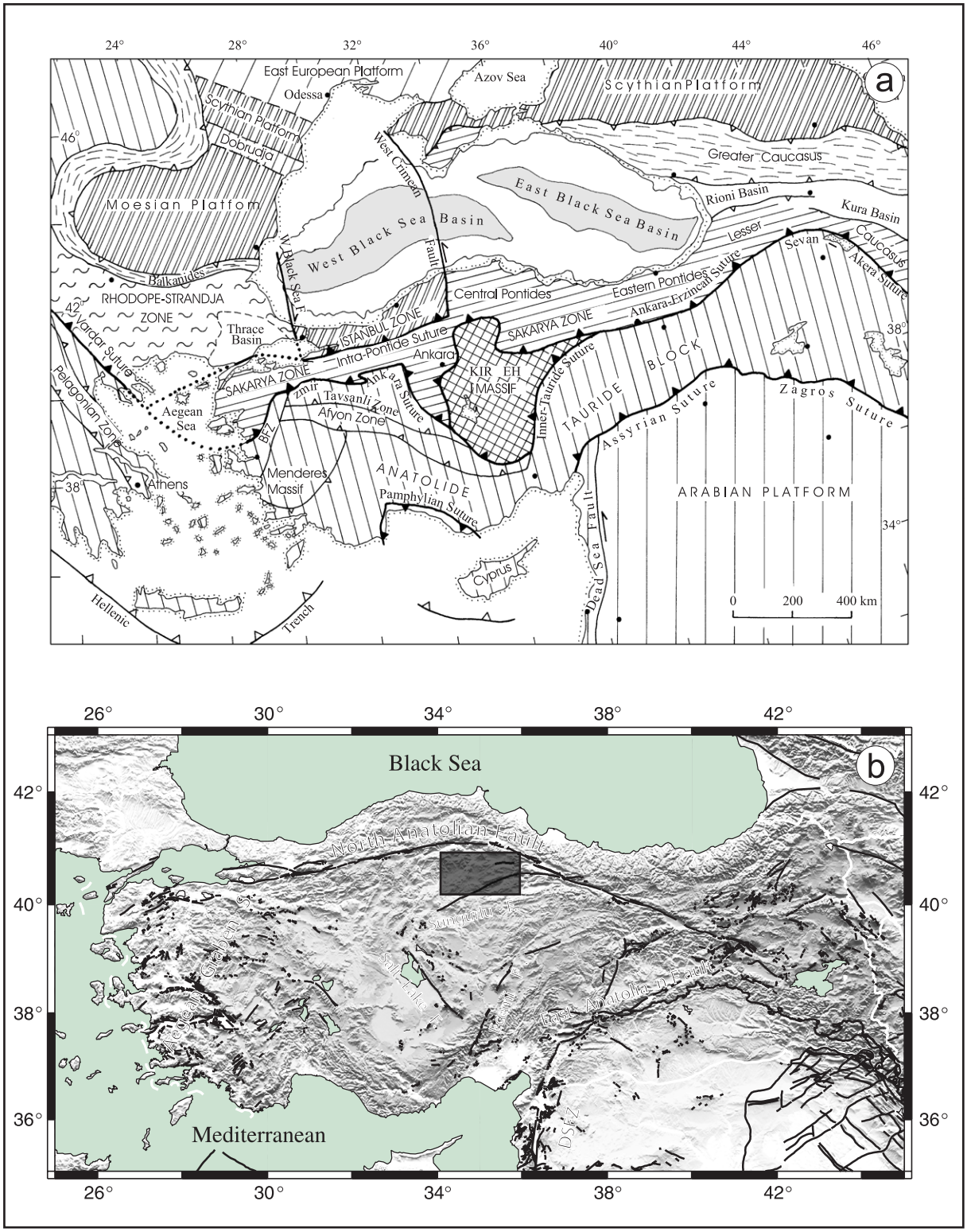

Fig. 1. (a) Palaeotectonic units of Turkey after Okay and Tüysüz (1999); (b) Major neotectonic features of Turkey (DSFZ, Dead Sea Fault Zone). Shaded box shows the study area.

broad zone of distributed deformation and the weak structure of the NASZ is evidenced by seismic activity, which is more prominent and distributed within the zone.

Within the NASZ, there are different offshoots (splines) that leave the main branch of the NAF and extend into the interior parts of Anatolia. Both the main branch and these offshoots divide the shear zone into dextral fault-bounded blocks. As a result of differential movements along the main branch and the offshoots, these fault-delimited blocks display different rotations as indicated by palaeomagnetic data. Where

observations are made in the central part of the NASZ, the shear-related clockwise rotations are found in areas as far south as 70–80 km from the main strand of the NAF, in contrast to earlier reports of no rotation (Platzman et al., 1994). Further west, around the western half of the Sea of Marmara, such rotations of Miocene and younger units are spread over a width of more than 100 km (Tapırdamaz and Yaltırak, 1997). In contrast, in the eastern part of the NASZ, the rotations are confined to a much narrower shear zone of some 15 km width (e.g. Tatar et al., 1995; Piper et al., 1997a).

In this study, we have collected Eocene volcanic rocks from different fault-delimited blocks in North Central Anatolia, in the southern part of the main branch of the North Anatolian Fault. The study area consists of several branches (splines) of the North Anatolian Fault and most of these branches are still active as indicated by earthquake activity during historical and instrumental periods (Ambraseys and Finkel, 1995). The goal of the study was to obtain and compare palaeomagnetic data from these fault-bounded blocks in order to understand the kinematics of block rotation.

2. Geological setting

The paleotectonic units of Turkey consist of six continental fragments: the Strandja Zone, the Istanbul Zone, the Sakarya Zone, the Anatolide–Tauride Block, the Kırşehir Block and the Arabian Platform (Fig. 1a; Şengör and Yılmaz, 1981; Şengör et al., 1982; Okay and Tüysüz, 1999). The first three zones are classically referred to as the Pontides and are separated from the Kırşehir Block and the Anatolide–Tauride Block by the İzmir–Ankara–Erzincan Suture. An important feature of the study area is the Çankırı Basin of Tertiary age which developed on both the Sakarya Zone and the Kırşehir Block and also on the İzmir–Ankara–Erzincan Suture separating these continental fragments. Tüysüz et al. (1995) indicate that the İzmir–Ankara–Erzincan branch of the Neo-Tethys, namely the İzmir–Ankara–Erzincan Ocean, opened during the Lias and started to close at the beginning of the middle Cretaceous through subduction of oceanic lithosphere along two or more north-dipping subduction zones. The northern subduction zone was along the southern margin of the Sakarya Continent. As a consequence of subduction along this zone, an ensialic magmatic arc, some fore-arc basins and a mélange belt developed. The second subduction zone, located to the south, gave rise to a mélange belt and an ensimatic arc developed on it. The central part of the Ankara–Erzincan Ocean closed by collision of the Kırşehir and the Sakarya Continents during the late Maastrichtian–early Eocene interval. As a result of this subduction and collision, mélange belts and ensimatic arc volcanics formed the İzmir–Ankara–Erzincan Suture between these continental fragments.

Our study area is located on the eastern part of the Sakarya Continent, known as the Tokat Massif, and is located to the east of the Çankırı Basin (Fig. 2). The Tokat massif was imbricated by south-vergent thrusts during the collisional period (Tüysüz, 1996). Cenomanian–Early Campanian mélange wedges were also emplaced onto the Sakarya Continent accretionary collage during this imbrication. Flat-lying Middle Eocene deposits cover the whole imbricated assemblage of the Tokat Massif and clearly postdate the imbrication.

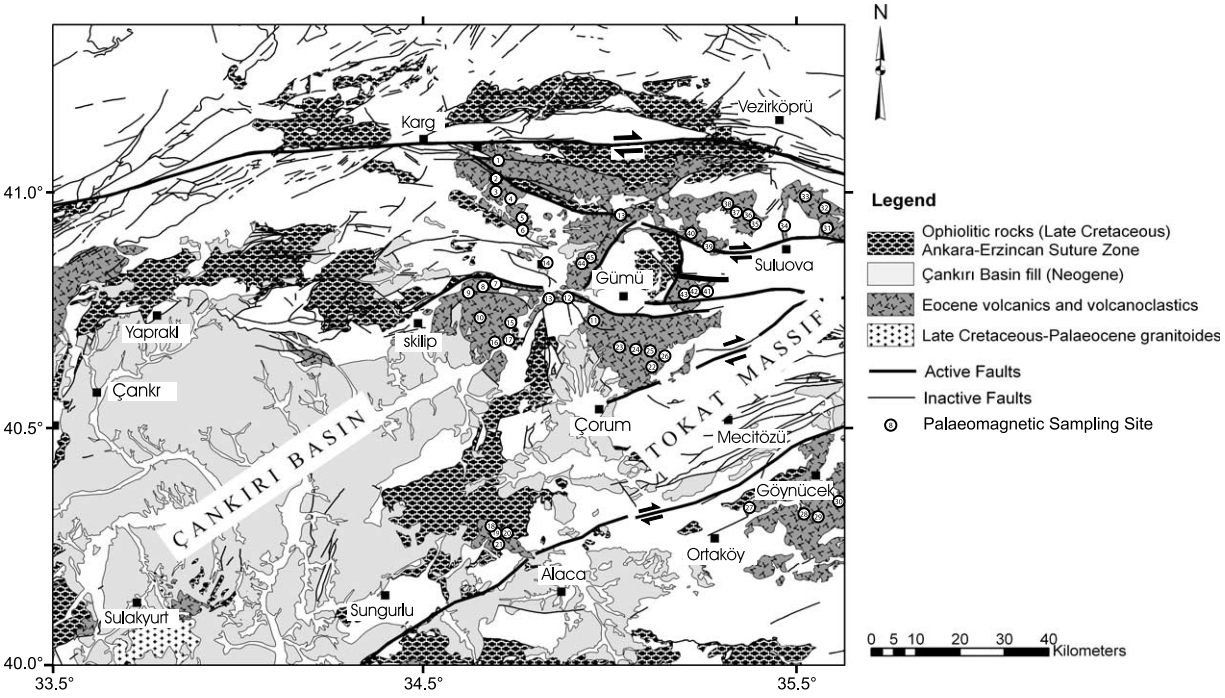

Fig. 2. Simplified geological map of the Çankırı Basin and the Tokat Massif. Open circles show the palaeomagnetic sampling sites and the numbers indicate site numbers in Table 1.

The Çankırı Basin to the east of the Tokat Massif began to develop as a fore-arc basin over the northward-subducting oceanic lithosphere during the late Cretaceous, and gradually changed into a post-collisional basin following collision of the Sakarya and Kırşehir continental blocks during the late Paleocene and early Eocene. The basin attained its maximum depth during the middle Eocene, and was then elevated by thrusting along its periphery. During the late Eocene–Oligocene period, regressive and subsequently continental clastics were deposited in the basin (Tüysüz et al., 1995; Tüysüz and Dellaloğlu, 1992, 1994; Görür et al., 1998).

In contrast to the Çankırı Basin, the Sakarya Zone remained as a positive area during the Maastrichtian–early Eocene interval (Tüysüz, 1996). At the end of the early Eocene, this belt was covered by a shallow marine sea which gave rise to deposition of Middle Eocene clastics and carbonates. Large amounts of post-collisional magmatic rocks, including lava, pyroclastics and small intrusives, are associated with these sedimentary rocks (Keskin et al., 2004). The thrusts which affected the pre-Miocene sequence of the Çankırı Basin are not seen in the Tokat Massif, except along its periphery, where there is a thrust zone representing the borders of the Tokat Massif with the Çankırı Basin to the west and the Ankara–Erzincan Suture to the south (Fig. 2). Middle Eocene and younger deposits are generally seen as flat-lying beds on the Tokat Massif, except in areas tilted by younger faults.

Both the Tokat Massif and the Çankırı Basin were affected by extensional and strike-slip tectonic regimes during the middle and late Miocene, respectively. During this period, the Çankırı Basin was an intermontane basin in which terrestrial clastics and evaporites were deposited. In addition, some longitudinal depressions, such as the Merzifon and Tosya basins, also formed and were filled with late Miocene to Quaternary sediments along the NAF. It is generally accepted that these basins opened during, or just before, the early evolution of the NAF.

We sampled Eocene volcanic rocks for this study. Palaeontological data from sedimentary rocks interlayered with the volcanic rocks indicate a middle Eocene age (Blumenthal, 1948; Avşar, 1991; Tüysüz and Dellaloğlu, 1992; Tüysüz, 1996). Platzman et al. (1994) obtained comparable ages from the same volcanic unit to the east of our study area (Tokat–Niksar region) using K–Ar whole rock analyses. They resolved ages ranging from 41.8 ± 1.3 to 45.3 ± 3.1 Ma, indicating a relatively short period of volcanic activity during the middle Eocene. Tectonic rotations recognized in Eocene units are comparable over a large area of Central Anatolia (Platzman et al., 1994; Tatar et al., 1996) and north of the NAF (Sarıbudak, 1989), and prove to be similar to rotations recognized in neotectonic rock units. This implies that major differential rotations were largely concentrated within the neotectonic period. Gürsoy et al. (2003) concluded that palaeomagnetic results from the palaeotectonic units of northern Anatolia yield declinations comparable with results from Late Miocene and younger units and suggest that the declination anomaly is attributable to rotation during the neotectonic regime. The magnitude of rotation south of the NAF is larger than the rotation in rocks of similar age to the north of the fault, indicating that differential rotation is occurring in continental blocks delimited by faults splaying into the Anatolian collage on the south side of the NAF.

In the light of these data, we decided that palaeomagnetic data from the Middle Eocene volcanic rocks could be used to compare vertical block rotations of different fault-bounded blocks. Areas not affected by post-Eocene compressional deformation far from the thrusts surrounding the Tokat Massif and displaying horizontal or low-dipping bedding or simply tilting due to faulting, were chosen as sampling locations. The dips of the beds in the sampling locations are mostly less than 25°.

The structure of the North Anatolian Fault and its branches in and around the study area are shown on Fig. 1b. The main active branch of the NAF forms the northern boundary of the westward moving Anatolian collage. Most of this fault was broken during the 1943 Tosya earthquake ($M = 7.6$, surface rupture was 260 km). The longest southern branch is the Sungurlu Fault which leaves the main branch in Niksar town to the east and extends southwestwards into the Kırşehir Block. The eastern part of this fault was broken during the 1939 Erzincan earthquake ($M = 7.9$, surface rupture was 370 km). The Çaldağ, Osmancık, Gümüş, Merzifon and Amasya blocks located between the Sungurlu Fault and the main branch of the NAF are separated from one other by secondary branches. Historical and instrumental records indicate that these secondary branches are also active (Eyidoğan et al., 1991; Ambraseys and Finkel, 1995; Ambraseys and White, 1997).

3. Field and laboratory methods

Sampling of the Middle Eocene volcanic rocks was designed to cover all of the fault-bounded blocks of the study area, except the Gümüş Block, where Eocene volcanics do not occur. Sampling locations are given on Fig. 2. Sites ORT1-4 are from andesitic lava flows on the Tokat Block. Sites OSM5-14, COM1-5 and SU1-4 belong to andesitic lava flows on the northern and southern parts of the Amasya Block. Sites KAM1-2, GHK4 and MER1-10 represent the Çaldağ Block to the south of the North Anatolian Fault. Sampling sites KAM3, OSM1-3 and GHK5-6 are located on the Osmancık Block. Finally, three sites GHK1-3 are located on the Merzifon Block. In each sampling location, at least seven independent cores were drilled using a portable motor and oriented by sun and magnetic compasses.

In the laboratory, cores were sliced into 2.54 cm length cylinders and natural remanent magnetization (NRM) was measured by using a spinner magnetometer. Some cores were subjected to progressive alternating field (AF) demagnetization in steps of 5–25 mT, then in steps of 10 mT, until directional behaviour ceased to be systematic. The other samples were subjected to thermal demagnetization in a MMTD60 demagnetizer; this was performed in steps of 50 °C from 0 to 100 °C, and then in steps of 25 °C to the Curie points of the magnetic minerals.

Table 1
Site mean palaeomagnetic results

Site number	Site name	N/n[a]	R[b]	α_{95}[c]	k[d]	D (in situ)	I (in situ)	D (tec. cor.)	I (tec. cor.)	Pol.[e]
Kamil										
1	KAM1	8/9	8	4.2	179.1	180	−29	187	−39	R
2	KAM2	6/8	5.9	7.5	79.8	162	−23	–	–	R
3	KAM3	9/9	8.5	13.1	22.1	188	−39	–	–	R
Osmancık										
4	OSM1	6/10	5.7	16.8	16.9	149	−58	–	–	R
5	OSM2	5/5	2.8	81.1	1.9	263	1	–	–	*N*
6	OSM3	8/9	7.8	10.1	31.3	240	−14	–	–	R
7	OSM4	9/9	8.7	9.3	31.8	239	−23	–	–	R
8	OSM5	7/9	6.8	11.7	27.8	194	−34	204	−25	R
9	OSM6	7/9	6.9	6.9	76.8	202	−55	219	−45	R
10	OSM7	7/9	5.8	11.7	43.8	185	−23	190	−47	R
11	OSM8	9/9	8.9	4.3	141.4	199	−23	212	−30	R
12	OSM9	8/8	7.9	5.7	95.5	258	−27	–	–	R
13	OSM10	6/7	6	6.7	101.4	196	−69	–	–	R
14	OSM11	7/8	6.9	7.5	66.5	173	−22	–	–	R
15	OSM12	8/8	7.9	5.4	108.1	192	−56	–	–	R
16	OSM13	8/9	6.8	12.5	24.3	195	−25	–	–	R
17	OSM14	9/9	8.9	4.9	111.4	231	−47	–	–	R
Sungurlu										
18	SU1	9/9	8.9	4.6	124.5	214	−37	–	–	R
19	SU2	9/9	8.9	6	73.6	224	−40	–	–	R
20	SU3	9/9	8.9	5.3	95.1	212	−62	–	–	R
21	SU4	7/9	6.8	10.4	34.9	200	−54	220	−38	R
Çorum										
22	COM1	5/7	4.9	9.1	71.1	177	−67	202	−68	R
23	COM2	9/9	8.9	6.7	59.6	213	−64	–	–	R
24	COM3	5/8	4.7	20.1	15.4	188	−58	–	–	*R*
25	COM4	9/9	8.9	3.4	225.4	206	−57	–	–	R
26	COM5	7/9	6.9	9.5	41.4	175	−41	184	−46	R
Ortaköy										
27	ORT1	8/8	7.9	6.3	77.5	137	−54	141	−39	R
28	ORT2	8/8	7.8	7.2	60.4	162	−54	–	–	R
29	ORT3	6/8	5.9	7.7	77.2	136	−47	149	−29	R
30	ORT4	8/9	6.9	23.8	6.4	184	52	–	–	*N*
Merzifon										
31	MER1	8/8	7.9	7.6	54.5	213	−30	223	−48	R
32	MER2	8/8	3.1	81.7	1.4	275	51	–	–	*N*
33	MER3	8/8	7.8	8.8	41	97	−20	82	−25	R
34	MER4	7/8	6.9	8.1	56.9	156	−29	–	–	R
35	MER5	5/8	4.8	17.2	20.6	22	−26	42	25	N
36	MER6	7/7	4.2	54.7	2.2	213	−23	–	–	*R*
37	MER7	8/8	7.8	8.7	41.9	177	−35	134	−53	R
38	MER8	8/9	4.6	53	2.1	331	9	–	–	*N*
39	MER9	8/8	8	4.4	162	51	13	45	10	N
40	MER10	10/10	5.2	52.2	1.7	84	−35	–	–	*R*
Gümüşhacıköy										
41	GHK1	7/7	6.8	12	26.3	157	−52	–	–	R
42	GHK2	9/9	8.9	5.4	91.9	93	−58	123	−47	R
43	GHK3	9/10	8.8	7.7	45.6	149	−58	–	–	R
44	GHK4	10/10	9.7	9.5	26.7	270	−59	252	−55	R
45	GHK5	6/9	5.7	18	14.8	196	−37	–	–	*R*
46	GHK6	7/9	6.8	9.9	37.9	199	−76	195	−52	R

[a] n the number of samples used to calculated the mean from a site population of N.
[b] R the resultant vector.
[c] α_{95} the radius of the cone of 95% confidence about the mean direction in degrees.
[d] k the Fisher precision parameter ($k=(n-1)/(n-R)$).
[e] Directions are classed as normal and reverse (N, R).

Orthogonal projections of the demagnetization data were produced in order to isolate components making up the NRM and calculate their directions by principal component analysis. Stereographic projections of the palaeomagnetic sites were also produced to show the mean remanant magnetization directions.

4. Palaeomagnetic study

Palaeomagnetic samples were collected from 46 Middle Eocene lavas from different blocks. Following standard palaeomagnetic techniques, nine sites were rejected due to their instability (Table 1). Seven examples of demagnetization

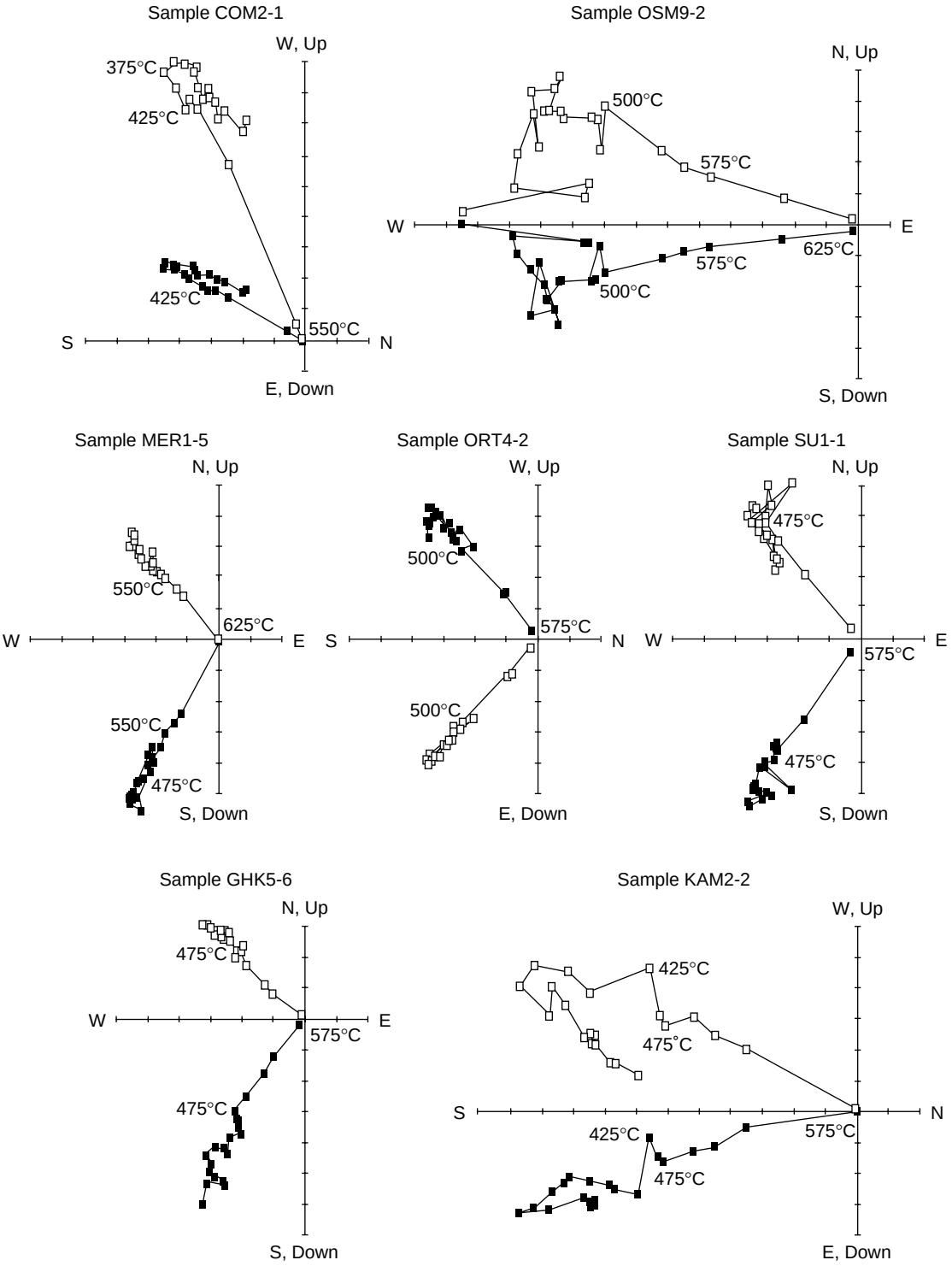

Fig. 3. The orthogonal projections illustrate behaviours of the remanence to progressive steps of thermal demagnetization as projections onto the horizontal (closed square) and vertical (open square) planes. Total NRM intensities are 24 (COM2-1), 17 (OSM9-2), 48 (MER1-5), 19 (ORT4-2), 15 (SU1-1), 44 (GHK5-6) and 10 (KAM2-2)$\times 10^{-5}$ $Am^{-2}\,kg^{-1}$. All directions are shown in situ.

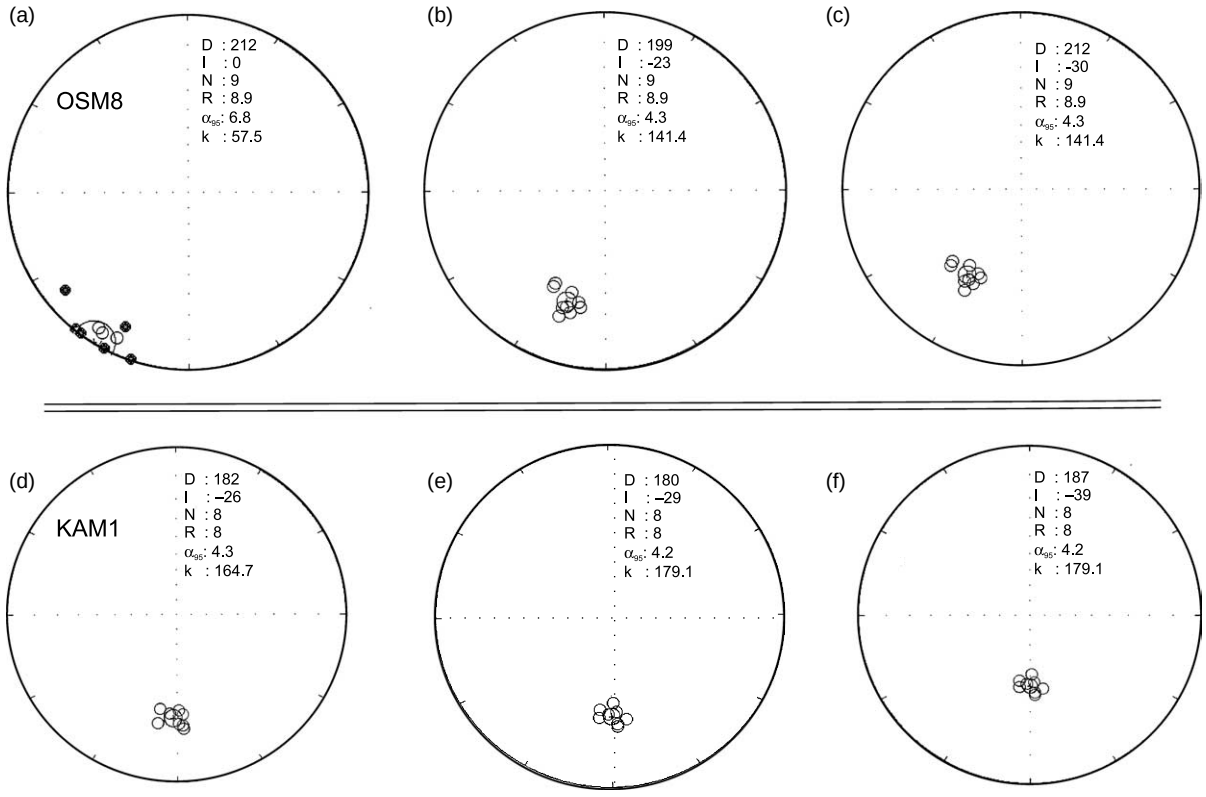

Fig. 4. Site mean directions for two palaeomagnetic sites (OSM8 and KAM1). Stereographic projections illustrate NRM directions (a, c), before tectonic correction (b, e), after tectonic correction (c, f) of remanent magnetization directions respectively from OSM8 and KAM1. Closed circles are upper-hemisphere projections and opened circles are lower-hemisphere projections.

results representative of the high quality of Characteristic Remanent Magnetization (ChRM) definition in these samples are shown in Fig. 3. This definition is preserved at site level with consistent groupings and α_{95} values mostly $<9°$ (Table 1).

Thermal demagnetization mostly isolates two and three component structures in magnetite (Fig. 3). ChRM typically is removed at temperatures ranging from 550 to 575 °C, close to the Curie point of magnetite. Hematite-held components are subtracted at higher temperatures (Fig. 3) and have the same direction as the magnetite ChRM.

Site mean magnetization directions were calculated using Fisher statistics and are illustrated on typical stereographic projections in Fig. 4. Tectonic corrections were applied and two examples of site mean directions (NRM, before and after tectonic correction) are given in Fig. 4.

5. Interpretation of palaeomagnetic results

Eocene volcanic rocks in North Central Anatolia have a common reversed polarity (Piper et al., 1996, 1997a; Tatar et al., 1995, 1996; Kaymakçı et al., 2003). In this study, similar reversed polarities are resolved from the Tokat Massif and 44 of 49 palaeomagnetic sites yield this polarity (Table 1). Since frequent reversals occurred during these times (Cande and Kent, 1995), these common reversed polarities appear to record a short term volcanic episode which is useful for identifying subsequent tectonic rotations.

Site mean palaeomagnetic directions (Table 1) with sector delineating cones of 95% confidence are given in Fig. 4 and illustrate good within-block consistency. As the middle Eocene and younger rocks of the study area have not been affected by important compressional deformation, they display low-dipping structure (average 25°), except the areas tilted due to fault-related deformations. This type of deformation is generally delimited to a narrow zone along the faults. We

Table 2
Summary of group mean palaeomagnetic results from this study

Blocks	D/I[a]	N/R[b]	α_{95}[c]	k[d]
Osmancık (OSM)	206/−40	7/6.9	12.7	23.7
Merzifon (MER)	223/−28	3/2.9	30	18
Sungurlu (SU)	219/−38	3/3	6.4	366.8
Çorum (COM)	202/−62	4/4	8.3	124.4
Gümüş (GHK)	142/−53	3/3	19.1	42.8
Ortaköy (ORT)	150/−41	3/2.9	22.6	30.7
Kamil (KAM)	188/−39	2/2	1.7	2173

Note: Mean reversed field direction (D/I: 191/−53.2) predicted for study area (40.75°N, 35°E) from the Apparent Polar Wander Path of Eurasia (Besse and Courtillot, 2002).

[a] D/I declination/inclination.

[b] N/R the number of sites/the resultant vector.

[c] α_{95} the radius of the cone of 95% confidence about the mean direction in degrees.

[d] k the Fisher precision parameter.

were prevented from sampling these areas to obtain the rotation of the blocks. Due to this structure of Eocene rocks, a fold test could not be conducted. We used strike and dip values of the alternating volcanic and sedimentary beds of the Middle Eocene unit for tectonic corrections. After the correction, we obtained a good consistency of site mean directions of each block, and we used the average of these directions (group mean) to interpret the tectonic rotations (Table 2). One exception was site MER3 from the Merzifon Block which was inconsistent (*D*/*I*: 82/−25) with another site in the same block. This inconsistency may be attributed to the transitional field.

Reference reverse polarity paleofield directions in the study area (40.75°N, 35°E) calculated from the mean poles for Europe (Besse and Courtillot, 2002) are *D*/*I*: 191°/−53.2° and block mean directions have compared with this predicted field direction in Eocene times. Blocks mean directions were calculated in order to compare the tectonic rotations of the fault-bounded blocks. Consistent groupings are found in six of the seven blocks (Table 2). Clockwise rotations are seen in Amasya, Osmancık, and some parts of the Çaldağ blocks while anticlockwise rotations are seen in the Tokat, Merzifon and Osmancık blocks (Fig. 5). Detailed descriptions of each block are given below:

The Tokat Block is delimited to the north by the dextral Sungurlu Fault. Seismic data and GPS measurements (Yavaşoğlu et al., 2004a,b) indicate that movement along this fault is very slow. Rotstein (1984) proposed a model for the westward motion of Anatolia consisting of a uniform, tight, anticlockwise rotation of a block approximated by the convex shape of the NAF as well as by faults which splay from it to the south. On the other hand, GPS measurements in Central Anatolia (i.e. the Tokat Block here) show anticlockwise rotation of this block in an Arabia-fixed reference frame (McClusky et al., 2000). In light of these data, it is concluded that the anticlockwise rotation of the west and southwestward escaping Anatolian plate, as evidenced by GPS measurements and anticlockwise rotation of three sites on the Tokat Block, record this rotation.

The Amasya Block is delimited by the Laçin Fault to the north and the Sungurlu Fault to the south. Three locations have been sampled on this block. One location was east of İskilip, within the Çankırı Basin. About 10 km east of this location, the ophiolitic belt representing the İzmir–Ankara–Erzincan Suture thrusts westward over Eocene deposits of the Çankırı Basin. The samples have been collected from both intrusive and extrusive volcanic bodies and the mean clockwise rotation is about 15° (Fig. 5). The second location is north of Çorum on the Tokat Massif and east of the ophiolitic belt. Here a large magmatic complex, the Eğercidağ Complex (Tüysüz, 1996) consisting of intrusives and extrusives, has been sampled and a mean rotation for the complex is determined as 11° clockwise. The third location is northeast of Sungurlu town, where a small intrusive volcanic unit has been sampled and a clockwise rotation of about 28° determined. The clockwise rotations of these three locations indicate rotation of the entire Amasya block. As this block is delimited by two dextral faults to the north and south, the results are consistent with the expected rotation of a continental block bounded by two dextral faults (McKenzie and Jackson, 1986; Lamb, 1994).

The Çaldağ Block is bordered by the main branch of the NAF in the north and the Merzifon Fault to the south. Here the Eocene volcanic rocks alternate with shallow marine clastics and are also intruded into them. Both clockwise and anticlockwise rotations are documented from this block.

The Osmancık, Gümüş and Merzifon blocks are bordered by the Laçin Fault in the south and the Merzifon Fault to the north. In contrast to the other blocks, the contacts between these three blocks are NE-trending faults delimiting the Gümüş Block in the middle (Fig. 5). The Merzifon Basin to the south of the Merzifon Fault is a complex pull-apart basin filled with Upper

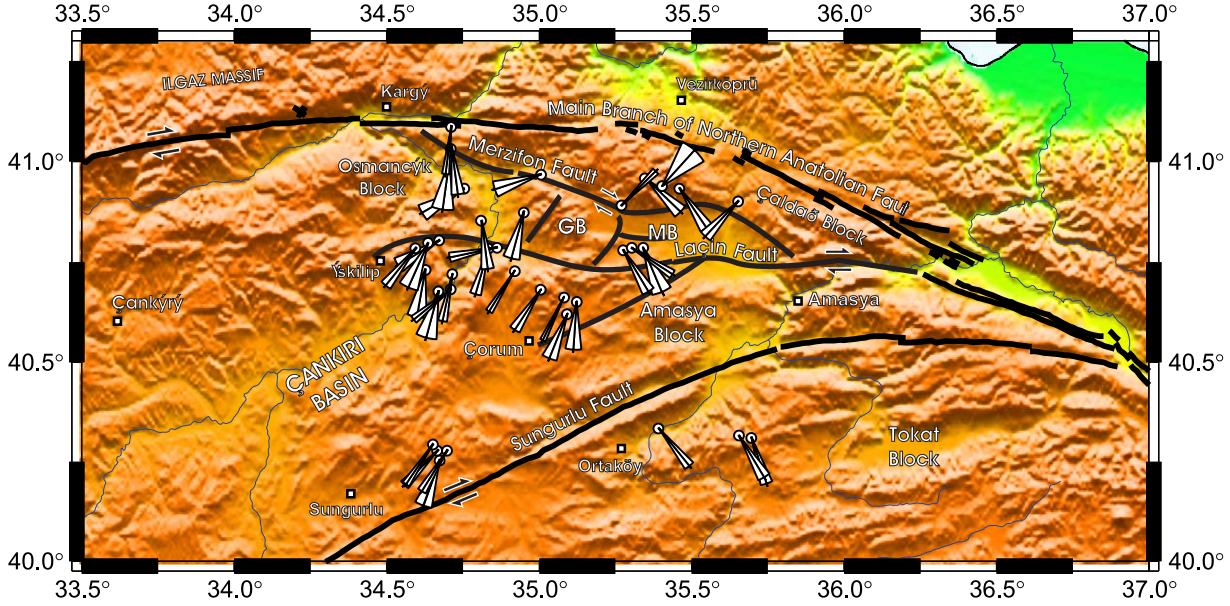

Fig. 5. Tectonic map of central Turkey showing the distribution of major faults active during the neotectonic regime and the declination of mean palaeomagnetic directions (see Table 1) with sectors delinating cones of 95% confidence. (GB, Gümüş Block; MB, Merzifon Block).

Miocene-Quaternary sediments. The Eocene volcanic rocks are seen in the western part of this block, close to the Gümüş Block where 49° degrees of anticlockwise rotations is resolved. There are no palaeomagnetic results for the Gümüş Block. Nevertheless a clockwise rotation is expected for this region by comparison with similar areas (Sarıbudak et al., 1990; Channell et al., 1996) along the NAF. Palaeomagnetic data from the Osmancık Block do not identify any important rotation in this region.

6. Discussion

Two different models have been proposed for the kinematics of vertical axis rotation in the upper crust, the continuum and discrete deformation models (Ron et al., 1984; Nelson and Jones, 1987; King et al., 1994; Piper et al., 1997b). The deformation is considered to be ductile and distributed over a wide area in the continuum models, while in discrete models the deformation causes rotation of internally undeformed continental blocks. As stated before by McKenzie and Jackson (1983) and Piper et al. (1997b), the deformation of continental lithosphere adjacent to intracontinental transform faults does not generally occur on a single fault, but is distributed over a zone. This zone of deformation is generally segmented into rigid continental blocks displaying simple to complex rotations. One of the deformation patterns created by the shearing stresses is block rotation around a vertical axis. It is generally considered that the most important reason for rotation of continental blocks is intracontinental strike-slip faults. Kinematically, in a simple shear system and homogenous media, a continental block between two dextral faults is expected to rotate clockwise and a continental block between two sinistral faults is expected to rotate anticlockwise (Nelson and Jones, 1987; Sonder et al., 1986). For example, Mino et al. (2001) described clockwise block rotations in contrast to the anticlockwise rotation of NE Japan and attributed this rotation to a dextral fault forming the boundary of the rotating domain. Iwaki and Hayashida (2003) and Itoh and Kimura (2004) also noted that the mountainous ranges of central Japan were rotated clockwise relative to the rest of the Japanese Islands, a sense of rotation opposite to that expected from collision of the Izu–Bonin Arc; this rotation is also attributed to differential block rotations between active dextral fault blocks. Beck et al. (1986) suggest that oblique convergence inducing dextral shear is responsible for the pattern of clockwise rotation in the Coastal Cordillera of Peru. Heimann and Ron (1993) identify anticlockwise rotation of fault blocks within the Korazim pressure ridge at the northern end of the Sea of Galilee by sinistral motion on the Jordan and Almagor fault segments of the Dead Sea Fault Zone.

Lamb (1987) indicates that the rate and sense of rotation depends on the aspect ratio (short axis/long axis) of the rotating elliptical block(s). The lower the aspect ratio of a block aligned parallel to the boundary, the higher the rate of rotation. On the other hand, if there is a single elongate block with an aspect ratio less than a critical value, it can remain essentially stationary. In our study area, maximum rotations of 49° anticlockwise and 61° clockwise were measured east and west of the Gümüş Block. The area to the east of the Gümüş Block is delimited by three faults to the west, south and north, and Quaternary deposits in the east. The shape of this area is rectangular with a short axis/long axis ratio of about 1.6. The structure of the area to the west of the Gümüş Block is not as clear as that in the east due to some small faults. This area rotated 61° clockwise. Both situations support Lamb's (1987) view that the shape of a block affects the rate of rotation.

Block rotations about a vertical axis have been widely studied in Anatolia and specifically along the NAF (Van der Voo, 1968; Sarıbudak et al., 1990; Platzman et al., 1994, 1998; Tatar et al., 1995, 2000, 1996; Piper et al., 1996, 1997a; Channell et al., 1996; Gürsoy et al., 1997, 1998). Sarıbudak et al. (1990) described a 212° clockwise rotation of the Almacık flake, a continental block delimited by two branches of the NAF, although Michel et al. (1995) refuted this conclusion. Similar clockwise rotation has also been described by Channell et al. (1996) around Reşadiye, on the eastern part of the NAF.

Based on palaeomagnetic data, Kissel et al. (2003) suggest that a large-scale anticlockwise rotation of the Anatolian Plate of some 25° has occurred since the collision between Anatolia and Arabia. Both the GPS data (Oral et al., 1995; Barka and Reilinger, 1997; McClusky et al., 2000) and our data from the Tokat Block (Fig. 5) support anticlockwise rotation; although we find that it is about 40°. Platzman et al. (1994, 1998) and Kissel et al. (2003) concluded that there was consistency of Eocene and Miocene palaeomagnetic results suggesting that the different Neotethyan blocks had accreted into a single coherent Anatolian Plate at least by the Miocene. These authors believe that uniform rotation of Anatolia started after the Miocene, and is still active as evidenced by GPS data (Oral et al., 1995; Barka and Reilinger, 1997; McClusky et al., 2000; Meade et al., 2002). However, more regional studies by Tatar et al. (2001) and Gürsoy et al. (2003) indicated that no coherent Anatolian Plate exists. Instead the zone of accreted terranes between the NAF and EAF is subject to distributed deformation and differential rotations. Our results also support discrete rotation instead of coherent block rotation.

7. Conclusions

One of the expected results of anticlockwise rotation of the Anatolian Plate is concave splines branching from the NAF (Fig. 1b). These splines can be compared with Cummings (1976)'s theoretical model based on Prandtl cells (Cummings, 1976; Şengör, 1979, 1980). One of the longest of these splines on the NAF is the Sungurlu Fault which leaves the main branch and extends southwestwards into the Kırşehir Block. This fault clearly follows a weak zone formed from ophiolitic rocks imbricated with continental slices (Tüysüz, 1993, 1996) and ends where it extends to the continental mass of the Kırşehir Block. In our study area, the Sungurlu Fault also forms the boundary between anticlockwise and clockwise rotated blocks. A 40° anticlockwise rotation of the southern block of the Sungurlu Fault is attributed to rotation of the Anatolian Plate.

The area between the Sungurlu Fault and the main branch of the NAF is dissected by active faults, two of which are important with respect to their earthquake activity, namely the Laçin and Merzifon faults. The Laçin Fault also divides into two splines to the south of the Merzifon pull-apart basin. These two splines delimit the Eğercidağ magmatic complex. Both the Laçin and Merzifon faults produced destructive earthquakes during the 1940s (Eyidoğan et al., 1991). In addition to the roughly E–W trending Laçin and Merzifon faults, there are also some roughly N–S trending faults in this area. The longest of these faults delimits the Gümüş Block and striation measurements indicate that both faults are dextral. Although there are no palaeomagnetic data to indicate the geometry of this block (Fig. 5), we infer that it has been rotated clockwise by the Merzifon and Laçin faults.

Palaeomagnetic results from the Çaldağ, Osmancık, Merzifon and Amasya blocks indicate predominant clockwise rotation. As all the faults delimiting these blocks are dextral, clockwise rotations are expected. Although rotation is predominantly clockwise, some results indicate anticlockwise rotation and could be explained by (a) pre-faulting deformation; (b) effects of unmapped small faults; (c) effects of non-vertical rotation due to opening of pull apart basins (i.e. the Merzifon pull-apart basin; (d) error in the tectonic correction and (e) the possibility that magnetizations are wholly, or in part, post-deformational.

The palaeomagnetic data presented in this paper support the idea that the Anatolian Plate is affected by discrete rotation instead of coherent block rotation.

Acknowledgements

This study has been supported by the Research Foundation of Istanbul Technical University (Project No: 1151). We thank Dr J.D.A. Piper for helpful reviews of the manuscript.

References

Ambraseys, N.N., Finkel, C.F., 1995. The Seismicity of Turkey and Adjacent Areas—a Historical Review, 1500–1800. Eren, İstanbul. 240 pp.

Ambraseys, N.N., White, D., 1997. The seismicity of the eastern Mediterranean region 550-1 BC: a re-appraisal. Journal of Earthquake Engineering 1, 603–632.

Avşar, N., 1991. Terziköy (Amasya) yöresinde bulunan bazı Nummulites türlerinin sistematik incelemesi. Geosound, Yerbilimleri. Science and Technology Bulletin on Earth Science, Adana 18, 111–127 (in Turkish with English abstract).

Barka, A., Reilinger, R., 1997. Active tectonics of the eastern Mediterranean region: deduced from GPS, neotectonic and seismicity data. Annali di Geophysica XL 3, 587–610.

Beck, M.E., Drake, R.E., Butler, R.F., 1986. Paleomagnetism of Cretaceous volcanic rocks from central Chile and implications for tectonics of the Andes. Geology 14, 132–136.

Besse, J., Courtillot, V., 2002. Apparent and true wander and the geometry of the geomagnetic field over the last 200 Myr. Journal of Geophysical Research 107 (B11), 2300.

Blumenthal, M.M., 1948. Bolu Civarı ile Aşağı Kızılırmak Mecrası Arasındaki Kuzey Anadolu Silsilelerinin Jeolojisi. Mineral Research & Exploration Bulletin Series B, Ankara (13), 265 (in Turkish with English abstract).

Cande, S.C., Kent, D.V., 1995. Revised calibration of the geomagnetic polarity timescale for the Late Cretaceous and Cenozoic. Journal of Geophysical Research 100 (B4), 6093–6095.

Channell, J.E.T., Tüysüz, O., Bektaş, O., Şengör, A.M.C., 1996. Jurassic–Cretaceous Paleomagnetism and Paleogeography of the Pontides. Tectonics 15 (1), 201–212.

Cummings, D., 1976. Theory of plasticity applied to faulting, Mojave Desert, southern California. Bulletin of the Geological Society of America 87, 720–724.

Eyidoğan, H., Utku, Z., Güçlü, U., Değirmenci, E., 1991. A Macro-seismic Catalogue of the Main Earthquakes of Turkey (1900–1988). Istanbul Technical University, Istanbul. 199 pp. (in Turkish).

Görür, N., Tüysüz, O., Şengör, A.M.C., 1998. Tectonic evolution of the Central Anatolian Basins. International Geological Review 40, 831–850.

Gürsoy, H., Piper, J.D.A., Tatar, O., Temiz, H., 1997. A palaeomagnetic study of the Sivas basin, central Turkey: crustal deformation during lateral extrusion of the Anatolian block. Tectonophysics 271, 89–105.

Gürsoy, H., Piper, J.D.A., Tatar, O., Mesci, L., 1998. Palaeomagnetic study of the Karaman and Karapinar volcanic complexes, central Turkey: neotectonic rotation in the south-central sector of the Anatolian block. Tectonophysics 299, 191–211.

Gürsoy, H., Piper, J.D.A., Tatar, O., 2003. Neotectonic deformation in the western sector of tectonic escape in Anatolia: palaeomagnetic study of the Afyon region, central Turkey. Tectonophysics 374, 57–79.

Heimann, A., Ron, H., 1993. Geometric changes of plate boundaries along part of the northern Dead Sea transform: geochronologic and palaeomagnetic evidence. Tectonics 12, 477–491.

Itoh, Y., Kimura, A., 2004. Paleomagnetism of a pyroclastic flow deposit and its correlative widespread tephra in central Japan: possible tectonic rotation since the late Pleistocene. The Island Arc 13, 110–118.

Iwaki, H., Hayashida, A., 2003. Palaeomagnetism of Pleistocene widespread tephra deposits and its implication for tectonic rotation in central Japan. The Island Arc 12, 46–60.

Kaymakçı, N., Duermeijer, C.E., Langereis, C., White, S.H., van Dijk, P.M., 2003. Oroclinal bending due to indentation: a paleomagnetic study for the early Tertiary evolution of the Çankiri Basin (central Anatolia, Turkey). Geological Magazine 140 (3), 343–355.

Keskin, M., Genç, Ş.C., Tüysüz, O., 2004. Tectonic setting and petrology of collision-related Eocene volcanism around the Çankırı basin, north central Turkey. 32nd International Geological Congress, Florence, Italy, August 20–28, Abstracts, Part 2, p. 1299.

Ketin, İ., 1966. Anadolu'nun tektonik birlikleri. Mineral Research & Exploration Bulletin, Ankara 66, 20–34 (in Turkish with English abstract).

King, G., Oppenheimer, D., Amelung, F., 1994. Block versus continuum deformation in the western United States. Earth and Planetary Science Letters 128, 55–64.

Kissel, C., Laj, C., Poisson, A., Görür, N., 2003. Paleomagnetic reconstruction of the Cenozoic evolution of the eastern Mediterranean. Tectonophysics 362, 199–217.

Lamb, S.H., 1987. A model for tectonic rotations about a vertical axis. Earth and Planetary Science Letters 84, 75–86.

Lamb, S.H., 1994. Behavior of the brittle crust in wide plate boundary zones. Journal of Geophysical Research 99, 4457–4483.

Le Pichon, X., Angelier, J., 1979. The Hellenic arc and trench system: a key to the neotectonic evolution of the eastern Mediterranean area. Tectonophysics 60, 1–42.

McClusky, S., Balassanian, S., Barka, A., Demir, C., Ergintav, S., Georgiev, I., Gürkan, O., Hamburger, M., Hurst, K., Kahle, H., Kastens, K., Kekelidze, G., King, R., Kotzev, V., Lenk, O., Mahmoud, S., Mishin, A., Nadariya, M., Ouzounis, A., Paradissis, D., Peter, Y., Prilepin, M., Reilinger, R., Şanlı, İ., Seeger, H., Tealeb, A., Toksöz, M.N., Veis, G., 2000. Global positioning system constraints on plate kinematics and dynamics in the eastern Mediterranean and Caucasus. Journal of Geophysical Research 105, 5695–5719.

McKenzie, D.P., Jackson, J.A., 1983. The relationship between strain rates, crustal thickening, paleomagnetism, finite strain and fault movements within a deforming zone. Earth and Planetary Science Letters 65, 182–202.

McKenzie, D.P., Jackson, J.A., 1986. A block model of distributed deformation by faulting. Geological Society (London) Journal 143, 349–353.

Meade, B.J., Hager, B.H., McClusky, S.C., Reilinger, R.E., Ergintav, S., Lenk, O., Barka, A., Özener, H., 2002. Estimates of seismic potential in the Marmara Sea region from block models of secular deformation constrained by global positioning system measurements. Bulletin of the Seismological Society of America 92, 208–215.

Michel, G.W., Waldhör, M., Neugebauer, J., Appel, E., 1995. Sequential rotation of streching axes, and block rotations: a structural and paleomagnetic study along the north Anatolian fault. Tectonophysics 243, 97–118.

Mino, K., Yamaji, A., Ishikawa, N., 2001. The block rotation in the Uetsu area, northern part of Niigata prefecture, Japan. Earth, Planets and Space 53, 805–815.

Nelson, M.R., Jones, C.H., 1987. Palaeomagnetism and crustal rotations along a shear zone, Las Vegas Range, southern Nevada. Tectonics 6, 13–33.

Okay, A.İ., Tüysüz, O., 1999. Tethyan sutures of northern Turkey. In: Durand, B., Jolivet, L., Hovarth, F., Séranne, M., (Eds.) The Mediterranean Basins: Tertiary Extension within the Alpine Orogen. Geological Society of London Special Publication 156, 475–515.

Oral, B., Reilinger, R., Toksöz, N.M., King, R., Barka, A., Kınık, I., Lenk, O., 1995. Coherent plate motion in the eastern Mediterranean continental collision zone. EOS January, 1–3.

Piper, J.D.A., Moore, J.M., Tatar, O., Gürsoy, H., Park, R.G., 1996. Palaeomagnetic study of crustal deformation across an intracontinental transform: the north Anatolian fault zone in northern Turkey. Geological Society Special Publication 105, 299–310.

Piper, J.D.A., Tatar, O., Gürsoy, H., 1997a. Deformational behaviour of continental lithosphere deduced from block rotations across the north Anatolian fault zone in Turkey. Earth and Planetary Science Letters 150, 191–203.

Piper, J.D.A., Stephen, J.C., Branney, M.J., 1997b. Palaeomagnetism of the Borrowdale and Eycott volcanic groups, English Lake District: primary and secondary magnetization during a single late Ordovician polarity chron. Geological Magazine 134 (4), 481–506.

Platzman, E.S., Platt, J.P., Tapırdamaz, M.C., Sanver, M., Rundle, C.C., 1994. Why are there no clockwise rotations along the north Anatolian fault zone? Journal of Geophysical Research 99, 21705–21715.

Platzman, E.S., Tapırdamaz, C., Sanver, M., 1998. Neogene anticlockwise rotation of central Anatolia (Turkey): preliminary palaeomagnetic and geochronological results. Tectonophysics 299, 175–189.

Ron, H., Freund, R., Garfunkel, Z., Nur, A., 1984. Block rotation by strike slip faulting: structural and palaeomagnetic evidence. Journal of Geophysical Research 89, 6256–6270.

Rotstein, Y., 1984. Counterclockwise rotation of the Anatolian block. Tectonophysics 108, 71–91.

Sarıbudak, M., 1989. New results and a palaeomagnetic overview of the Pontides in northern Turkey. Geophysical Journal International 99, 521–531.

Sarıbudak, M., Sanver, M., Şengör, A.M.C., Görür, N., 1990. Palaeomagnetic evidence for substantial rotation of the Almacık flake within the north Anatolian fault zone, NW Turkey. Geophysical Journal International 102, 563–568.

Şengör, A.M.C., 1979. The north Anatolian transform fault: its age, offset and tectonic significance. Journal of the Gelogical Society of London 136, 269–282.

Şengör, A.M.C., 1980. Türkiye'nin Neotektoniğinin Esasları (Principles of Neotectonics in Turkey). Geological Society of Turkey Conference Series, Ankara 2, 40.

Şengör, A.M.C., Yılmaz, Y., 1981. Tethyan evolution of Turkey: a plate tectonic approach. Tectonophysics 75, 181–241.

Şengör, A.M.C., Yılmaz, Y., Ketin, İ., 1982. Remnants of a pre-late Jurassic ocean in northern Turkey: fragments of Permo-Triassic Paleo-Tethys? Reply: Geological Society of America Bulletin 93, 932–936.

Şengör, A.M.C., Tüysüz, O., İmren, C., Sakınç, M., Eyidoğan, H., Görür, N., Le Pichon, X., Rangin, C., 2005. The north Anatolian fault: a new look. Annual Review of Earth and Planetary Sciences 33, 37–112.

Sonder, L.J., England, P.C., Houseman, G.A., 1986. Continuum calculations of continental deformation in transcurrent environments. Journal of Geophysical Research 91, 4797–4810.

Tapırdamaz, C., Yaltırak, C., 1997. Trakya'da Senozoyik volkaniklerinin paleomanyetik özellikleri ve bölgenin tektonik evrimi. Mineral Research & Exploration Bulletin 119, 27–42 (in Turkish with English abstract).

Tatar, O., Piper, J.D.A., Park, R.G., Gürsoy, H., 1995. Paleomagnetic study of block rotations in the Niksar overlap region of the north Anatolian fault zone, central Turkey. Tectonophysics 244, 251–266.

Tatar, O., Piper, J.D.A., Gürsoy, H., Temiz, H., 1996. Regional significance of Neotectonic counterclockwise rotation in central Turkey. International Geology Review 38, 692–700.

Tatar, O., Piper, J.D.A., Gürsoy, H., 2000. Palaeomagnetic study of the Erciyes sector of the Ecemiş Fault Zone: neotectonic deformation in the southern part of the Anatolian block. In: Bozkurt, E., Winchester, J.A., Piper, J.D.A., (Eds.) Geological Society of London, Special Publication 173, 423–440.

Tatar, O., Gürsoy, H., Piper, J.D.A., 2001. Differential neotectonic rotations in Anatolia and Tauride arc: palaeomagnetic investigations of the Erenlerdağ complex and Isparta volcanic district, south-central Turkey. EUG XI, Symposium LS03 Integrated Tectonic Studies of the Evolution of the Tethyan Orogenic Belt in the Eastern Mediterranean Region, April, Strasbourg, France, 322.

Tüysüz, O., 1993. Karadeniz'den Orta Anadolu'ya bir Jeotravers: Kuzey Neo-Tetisin Tektonik evrimi. Turkish Association of Petroleum Geologists Bulletin 5 (1), 1–33 (in Turkish with English abstract).

Tüysüz, O., 1996. Amasya ve çevresinin jeolojisi. 11th Petroleum Congress and Exhibition of Turkey, Proceedings, Geology, Turkish Association of Petroleum Geologists/UCTEA Chamber of Petroleum Engineers/UCTEA Chamber of Geophysical Engineers, 32–48 (in Turkish with English abstract).

Tüysüz, O., Dellaloğlu, A.A., 1992. Çankırı havzasının tektonik birlikleri ve jeolojik evrimi. Ninth Petroleum Congress and Exhibition of Turkey, Proceedings, Geology, Turkish Association of Petroleum Geologists/UCTEA Chamber of Petroleum Engineers/UCTEA Chamber of Geophysical Engineers, 333–349 (in Turkish with English abstract).

Tüysüz, O., Dellaloğlu, A.A., 1994. Orta Anadolu'da Çankırı Havzası ve çevresinin erken Tersiyer'deki paleocoğrafik evrimi. 10th Petroleum Congress and Exhibition of Turkey, Proceedings, Geology, Turkish Association of Petroleum Geologists/UCTEA Chamber of Petroleum Engineers/UCTEA Chamber of Geophysical Engineers, 56–76 (in Turkish with English abstract).

Tüysüz, O., Dellaloğlu, A.A., Terzioğlu, N., 1995. A magmatic belt within the Neo-Tethyan suture zone and its role in the tectonic evolution of northern Turkey. Tectonophysics 243, 173–191.

Van der Voo, R., 1968. Paleomagnetism and the Alpine tectonics of Eurasia, Part IV, Jurassic, Cretaceous and Eocene pole positions from NE Turkey. Tectonophysics 6, 251–269.

Yavaşoğlu, H., Rüzgar, G., Baykal, O., Bilgi, S., Çakmak, R., Erden, T., Ergintav, S., İnce, C.D., Karaman, H., Tarı, E., Tarı, U., Tüysüz, O., 2004. GPS measurements along the North Anatolian Fault Zone on the Mid-Anatolia segment. Fifth International Symposium on Eastern Mediterranean Geology, 14–20 April, Thessaloniki, Greece, vol. 2, 904–907.

Yavaşoğlu, H., Rüzgar, G., Tarı, E., Baykal, O., Erturaç, M.K., Çakmak, R., Erden, T., Ergintav, S., İnce, C.D., Karaman, H., Tarı, U., Tüysüz, O., 2004. GPS measurements on the Western Marmara of North Anatolian Fault segment. Fifth International Symposium on Eastern Mediterranean Geology, 14–20 April, Thessaloniki, Greece, vol. 2, 901–903.